

Preparation of Eosin Y/Graphene Oxide Modified Glassy Carbon Electrode as a Sensing Platform for Dopamine and Epinephrine Detection

Shengbiao Zheng, Yu Liu, Jing Liu, Jing Tang*

College of Chemistry and Material Engineering, Anhui Science and Technology University, 233000, Bengbu, Anhui Province, China

*E-mail: zhengtang102@163.com (Tang Jing)

Received: 5 January 2020 / *Accepted:* 2 March 2020 / *Published:* 10 April 2020

The electrodeposition of eosin Y (EY) on graphene oxide (GO) modified glassy carbon electrode (GCE) was performed and the modified platform applied for the simultaneous determination of dopamine (DA) and epinephrine (EP). The EY/GO modified GCE was characterized using electrochemical impedance spectra. The modified electrode exhibited excellent electroanalytical performance for DA and EP by cyclic voltammetry due to the synergistic effect of the good electrical conductivity of GO and electrochemical activity of EY. The linear responses were found by differential pulse voltammetry (DPV) between 0.2 and 100 μM concentration range for DA and EP, with detection limits of 50 nM for DA and 30 nM for EP ($S/N = 3$), respectively. Further experiments were investigated for electrode selectivity, stability and reproducibility. In addition, in order to evaluate electrochemical activities for this proposed electrode, the simultaneous determination of DA and EP at EY/GO/GCE was explored in diluted human urine samples.

Keywords: eosin Y; graphene oxide; dopamine; epinephrine; modified electrode

1. INTRODUCTION

Dopamine (DA) and epinephrine (EP), as the class of catecholamines, are typical neurotransmitters that help cells transmit pulses of chemicals and relate to large variety of physiological illnesses [1]. In recent years, monitoring DA and EP in human blood plasma and urine attracted great attention because they can be signaling the emergence of various diseases such as Parkinson's disease, schizophrenia and HIV infection [2-5]. Hence, the development of analytical techniques for selective and sensitive determination is very important. A large number of methods, such as high-performance liquid chromatography [6], spectrophotometry [7] and electrochemistry [8,9], are available for the detection of EP and DA. Among all, electrochemical methods are considered to be the most preferred

methods attribute to its distinct advantages of simplicity, reproducibility and cost efficiency. However, DA and EP have similar structure and usually coexist in real samples. The recognition and detection of them using bare solid electrode is difficult due to the overlap of potentials. Thus, some advanced materials modified electrode is expected for the determining of DA and EP.

As the important member of the carbon based materials, graphene, which consists of 2D structures with sp^2 -bonded carbon atoms in a hexagonal configuration, is ideal candidate material for electrochemical sensors attribute to its excellent conductivity, high surface area, biocompatibility, and robustness [10,11]. Moreover, graphene oxide (GO), which is a derivative of graphene, owns the excellent properties of graphene and possesses other advantages including hydrophilicity, controllable electronic properties and multiple oxygen moieties [12,13]. Recently, GO has attracted tremendous attention in the field of electrochemical sensors [14-19]. For example, the graphene modified electrode synthesized chemically by Wang et al. [19] was successfully employed in selective detection of DA in presence of AA. Graphene and related derivatives with large surface area act excellent carrier to load more active probes for molecules binding, giving significant amplification on the electrochemical sensing signals. Nowadays, conducting polymers can be combined with GO to fabricate novel conducting composites for improving the conductivity of GO in electrochemical applications [19].

Organic molecules owing to their good stability, reproducibility and more active sites can be applied for conducting polymers to modify electrodes for sensitive determination of morin, TBHQ, hydroquinone and catechol [20-22]. Eosin Y (2', 4', 5', 7'-tetrabromofluorescein disodium salt) is a xanthene dye, which has been applied in the field of laser dye, fluorescent probe, biological stain, sensitizer and electrochemical sensors [23-30]. He *et.al* [28] discovered that eosin Y modified GCE enlarged the surface area of electrode and reduced the oxidation overpotential to HQ and CC. Our group [29] have prepared the eosin Y film modified electrode, which showed excellent electrocatalytic activity towards the oxidation of TBH₂Q and BHA.

Herein, inspired from the excellent characteristics of GO and eosin Y, a novel modified electrode combining GO and eosin Y was fabricated by electrodepositing eosin Y on the GO/GCE matrix, which was obtained by casting a certain amount of well-dispersed GO suspension onto a bare GCE. Cyclic voltammetry (CV) and differential pulse voltammetry (DPV) were used to investigate the electrochemical performance of EY/GO/GCE. This hybrid combines the properties of GO and eosin Y, which shows a high catalysis performance for DA and EP.

2. MATERIALS AND METHODS

2.1 Materials

All chemicals were of analytical reagent grade and used as received, with no further purification. Eosin Y (EY) was received from Sigma-Aldrich (USA). Graphite was obtained from XFNANO Materials Tech Co., Ltd. Dopamine (DA) and epinephrine (EP) were provided by Aladdin Chemical Reagent Co. Ltd. All other chemicals were of analysis grade from Shanghai Chemical Reagent Co., Ltd (China). Phosphate buffer solution with different pH values was prepared by mixing an appropriate quantity of 0.1M NaH₂PO₄, Na₂HPO₄, H₃PO₄ and NaOH.

2.2 Apparatus

The electrochemistry measurements were carried out on CHI 660E electrochemical working station (Shanghai, China). Electrochemical impedance spectroscopy (EIS) were recorded with the frequency range from 0.1 Hz to 10 kHz at 0.25V. A three electrode cell were used to perform cyclic voltammetry (CV), linear sweep voltammetry (LSV) and differential pulse voltammetry (DPV) techniques at room temperature.

2.3 Fabrication of GO and EY/GO modified electrode

Graphene oxide was prepared by Hummers' method [31] from natural graphite powder. The GCE was cleaned with chamois leather containing alumina slurry (0.3 and 0.05 μm), and then it was cleaned with $\text{C}_2\text{H}_5\text{OH}$ and doubly distilled water each for 1 min ultrasonically, respectively. Then, the electrode was conducted by CV between -0.4 and 1.6 V in $0.1 \text{ mol}\cdot\text{L}^{-1}$ H_2SO_4 at $100 \text{ mV}\cdot\text{s}^{-1}$ until reached a steady state. GO suspension was fabricated by dispersing 4 mg of GO in 2 mL DMF by ultrasonication for 1 h to obtain a brown suspension. 4 μL of the GO suspension was dropped onto the prepared GCE and then dried to obtain a GO modified electrode, denoted as GO/GCE. Then, the EY/GO/GCE was obtained by electrodeposited eosin Y film on the GO/GCE. The eosin Y film in $0.1 \text{ mol}\cdot\text{L}^{-1}$ of phosphate buffer solution ($\text{pH} = 7.0$) containing $1.0\times 10^{-3} \text{ mol}\cdot\text{L}^{-1}$ eosin Y was prepared on the surface of the GO/GCE by electrodeposited with a scanning rate of $100 \text{ mV}\cdot\text{s}^{-1}$ from -1.6 to 1.5 V for 15 cycles [28, 29].

2.4 Detection of DA and EP in spiked human urine

Human urine samples, obtained from healthy volunteers, were diluted 50 times (by volume) with 0.1 M phosphate buffer solution ($\text{pH}=6.0$). Spiked urine samples were obtained by preparing 9 mL of diluted urine with known amounts of 1 mL DA or EP solution. The peak currents of the spiked urine samples were recorded. Recovery tests were conducted by DPV under optimized conditions.

3. RESULTS AND DISCUSSION

3.1 Characterizations of modified electrode

Fig. 1 shows the successive cyclic voltammograms (CVs) for the electrodeposition of 1 mM eosin Y at the bare GCE and GO modified GCE in phosphate buffer solution ($\text{pH} 7.0$). As seen, the eosin Y molecules were reduced to free radicals during the electrodeposited process and rapidly combined with the electrode surface [28, 29, 32]. The electrochemical process for EY^{2-} can be summarized in scheme 1. Meanwhile, the background current of GO/GCE was much higher than that of bare GCE, which mean that GO modified electrode had better electrochemical performance with higher electrocatalytic activity and more electroactive sites to the electrodeposition of eosin Y.

Electrochemical impedance spectroscopy (EIS) spectra can be assess the electrochemical properties of the different electrodes (bare GCE, GO/GCE, EY/GCE and EY/GO/GCE) in $[\text{Fe}(\text{CN})_6]^{3-}$

⁴⁻ system as a redox probe. The interfacial charge transfer resistance (R_{ct}) was equal to the diameter of the semicircle in the EIS spectra. As shown in Fig. 2, the R_{ct} value of bare GCE was estimated to be 600 Ω . When GO or EY was introduced on bare GCE, the R_{ct} value significantly decreased that of bare GCE, suggesting the high electron conductivity of GO and eosin Y materials. Moreover, the Nyquist plot of EY/GO/GCE was an almost straight line attribute to the synergistic effect of GO and eosin Y. The improved electrochemical characteristic implied that EY/GO/GCE could be a promising candidate for sensing applications.

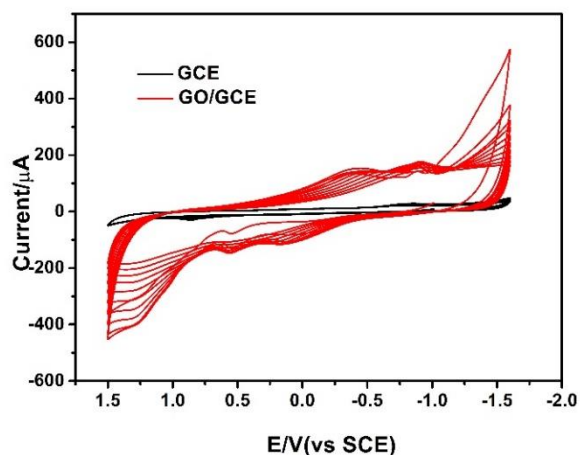
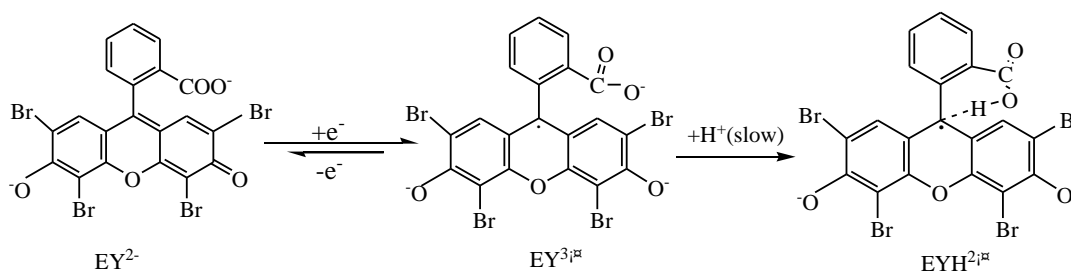


Figure 1. The successive CVs for the electrodeposition of 1 mM eosin Y at the GCE and GO/GCE



Scheme 1. Redox reactions of eosin Y[29]

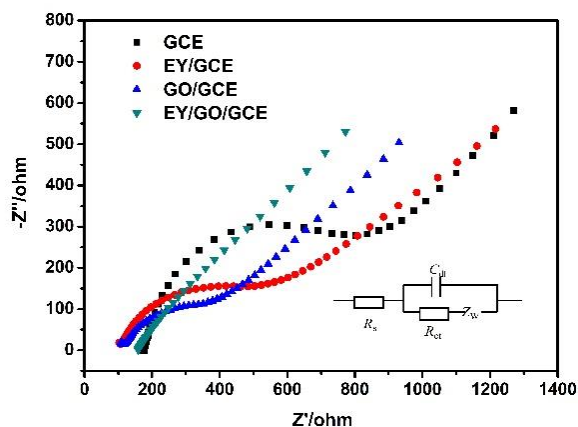


Figure 2. Nyquist plots of bare GCE, GO/GCE, EY/GCE and EY/GO/GCE with frequency range of 0.1–10⁵ Hz, a bias potential of 0.25 V vs. SCE. Inset: Randle equivalent electrical circuit.

3.2 Electrochemical responses of DA and EP at EY/GO/GCE

To exploit the potential application of the EY/GO/GCE, the electrochemical behaviors of DA (Fig. 3a), EP (Fig. 3b) and simultaneous detection of EP and DA (Fig. 3c) were studied on the EY/GO/GCE in 0.1 M phosphate buffer solution with pH value of 6.0 by cyclic voltammetry (CV). For comparison, the CV was conducted at bare GCE, GO/GCE and EY/GCE. As seen in Fig 3a, DA displayed a pair of redox peaks ($\Delta E_p=117$ mV) with the cathodic peak current of $2.78 \mu\text{A}$ at the bare GCE. The CV of DA at GO/GCE or EY/GCE has a couple of redox peaks and the potential difference of their peaks (ΔE_p) was decreased. Moreover, the peak intensity was remarkably increased, which can be attributed to the large specific area of GO and the electrocatalytic performance of EY. As for EY/GO modified electrode, the sharp cathodic peak current of $24.56 \mu\text{A}$ was observed, which was nearly 9-fold larger than that of the bare GCE. The outstanding enhanced electrocatalytic characteristic might be due to the synergistic effect of EY and GO.

The similar results for the electrochemical reaction of EP were also investigated in Fig. 3b. Only a small cathodic peak of EP was found at the GCE. Compared with the bare GCE, a pair of peaks of EP at GO/GCE and EY/GCE were observed, the cathodic peak potential located at -0.170 V and -0.164 V at GO/GCE and EY/GCE, respectively, and the peak currents were about $3.74 \mu\text{A}$ and $4.79 \mu\text{A}$. The obviously largest peak current (about $30.58 \mu\text{A}$) at EY/GO/GCE.

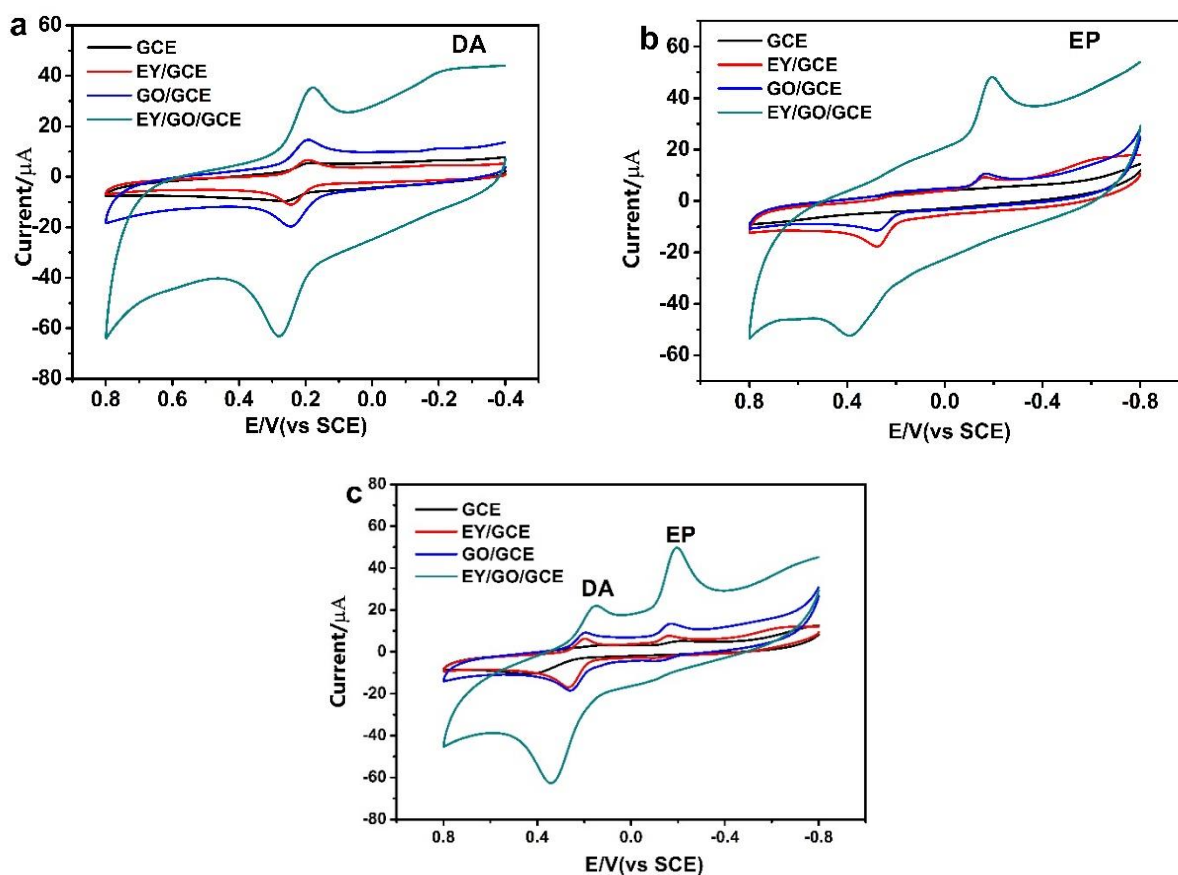


Figure 3. CVs of 0.1 mM of DA (a), 0.1 mM EP (b) and a mixture of 0.1 mM DA and 0.1 mM EP (c) at bare GCE, GO/GCE, EY/GCE and EY/GO/GCE in 0.1 M (pH 6.0) phosphate buffer solutions at scan rate: 100 mV/s.

The simultaneous detection of EP and DA were also conducted (Fig. 3c). At bare GCE, two oxidation peaks for DA (0.145 V) and EP (-0.222 V) with low current intensity were observed. When the GO or EY was modified on the GCE, the cathodic peak currents of EP and DA increased significantly and the cathodic peak potentials were positively shifted. Compared with the other electrodes, the reductive of EP and DA at EY/GO/GCE exhibited significantly increased current signals. Moreover, two separated reduction peaks corresponding to EP (-0.195 V) and DA (0.147 V) were obtained. A separation of 342 mV in reduction peak potentials was achieved, it is similar to the method reported (357 mV) [33]. The hybrid of GO and EY with high conductivity may offer more active sites and high surface area, which might be beneficial of the electrocatalysis. Moreover, the enhanced current signals could also result from the fact that the synergistic effect of GO and EY might be increase the electrochemical adsorbing amount of DA and EP. Overall, the GO and EY hybrid possess the superior performance toward electrochemical reaction of DA and EP.

3.3 Effect of phosphate buffer solution pH

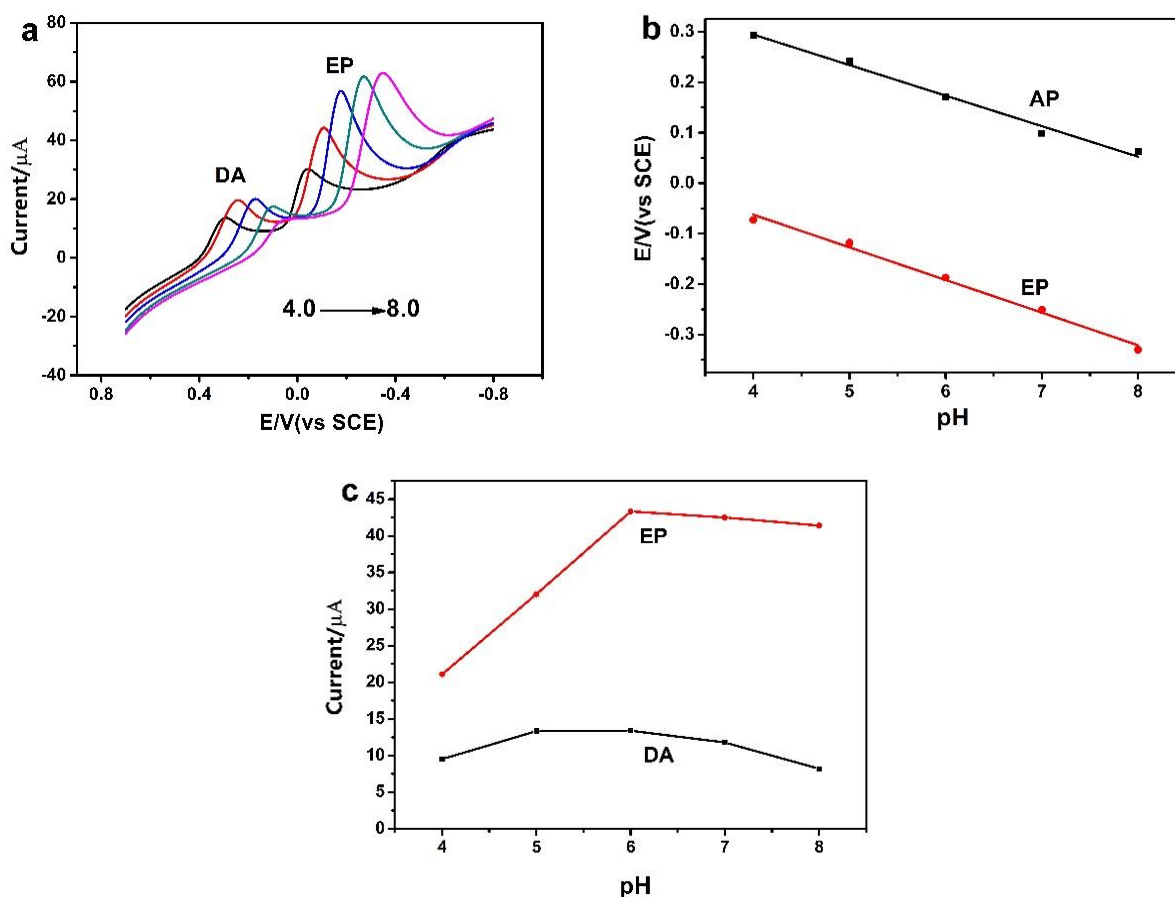


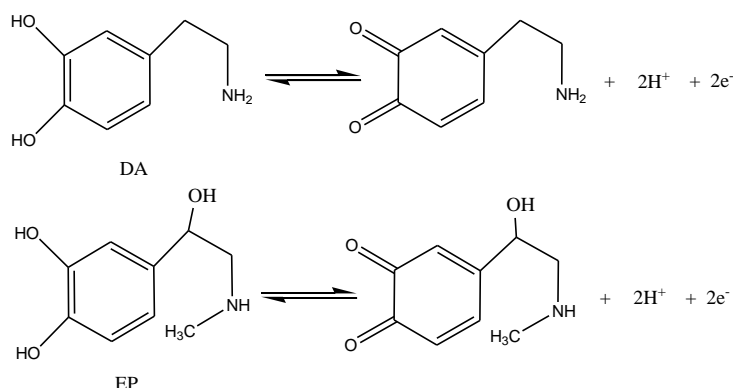
Figure 4. (a) LSV curves of 0.1 mM DA and 0.1 mM EP with different pH at EY/GO/GCE at scan rate of 100 mV/s. (b) Effect of pH on peak potentials for reduction of DA and EP. (c) Effect of pH on peak currents.

The proton is usually involved in the electrochemical reactions of many organic compounds. Therefore, LSV test was employed to investigate the effect at EY/GO/GCE with pH values ranging from 4.0 to 8.0 in 0.1 M phosphate buffer solutions containing 0.1 mM DA and 0.1 mM EP (Fig. 4a). As shown in Fig. 4b, the potential moved to lower potentials as pH was increased, indicating that the proton participated in the electrochemical reaction [34].

It was found that the potentials of reduction peaks (E_{pc}) of DA and EP was linear with pH value ranging from 4.0 to 8.0. The linear regression equations were $E_{pc} (V) = 0.5375 - 0.061 \text{ pH}$ ($R = 0.985$) for DA and $E_{pc} (V) = 0.1975 - 0.064 \text{ pH}$ ($R = 0.990$) for EP, respectively. According to equation:

$$\frac{dE_p}{dpH} = \frac{2.303mRT}{nF}$$

wherein m and n are the number of the protons and electrons, respectively. The value of m/n was calculated to be 1.03 (≈ 1) for DA and 1.08 (≈ 1) for EP from the slope of the E_p -pH plot, demonstrating that the electrochemical redox reaction of two compounds at EY/GO/GCE underwent a two electron and two proton process, consistent with other previous reports [35,36]. According to the experimental results and the literature [37], the reasonable reaction mechanisms of DA and EP at EY/GO/GCE were proposed as follows:



Moreover, the relationship between the reduction peaks currents and pH of EP and DA were displayed in the Fig. 4c, the peaks currents of EP and DA reached the highest value at pH 6.0. Therefore, pH 6.0 was applied for the detection of two compounds at EY/GO/GCE.

3.4 Effect of scan rate

The CVs of 0.1 mM DA and 0.1 mM EP at EY/GO/GCE at various scan rates were shown in Fig. 4a and c. The dependence of CVs of DA and EP on the scan rate (v) was shown in the Fig. 4b and d. It was found that all the peak currents (I_p) were proportional to the scan rate (v) at EY/GO/GCE over the range from 60 to 340 mV s^{-1} . Their linear regression equations can be expressed as: $I_{pa} (\mu\text{A}) = -0.1431v (\text{mV}\cdot\text{s}^{-1}) - 7.688$ ($R = 0.972$) and $I_{pc} (\mu\text{A}) = 0.0856v (\text{mV}\cdot\text{s}^{-1}) + 40.90$ ($R = 0.971$) for EP, $I_{pa} (\mu\text{A}) = -0.1238v (\text{mV}\cdot\text{s}^{-1}) - 34.60$ ($R = 0.981$) and $I_{pc} (\mu\text{A}) = 0.1241 (\text{mV}\cdot\text{s}^{-1}) + 9.433$ ($R = 0.993$) for DA, respectively, suggesting that the electrode reactions of the two compounds at EY/GO/GCE were absorption-controlled processes [38].

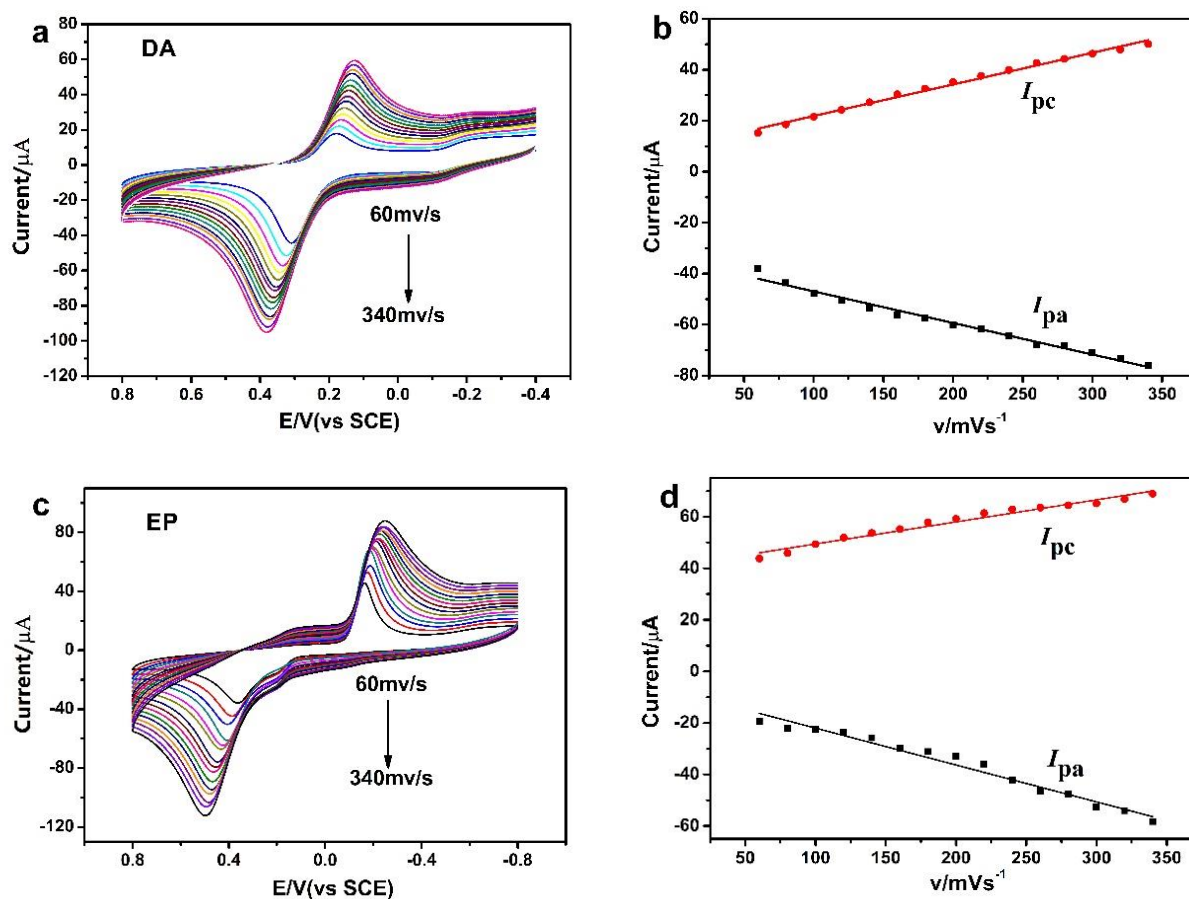


Figure 5. CVs of 0.1 mM DA (a) and 0.1 mM EP (c) at EY/GO/GCE with different scan rates (60, 80, 100, 120, 140, 160, 180, 200, 220, 240, 260, 280, 300, 320 and 340 mV s^{-1} , respectively). Plot of the peak currents (I_p) of DA (b) and EP (d) versus scan rates (v).

3.5 Analytical performance

To verify and compare the electrochemical performances of EY/GO modified electrode with and without the potential interference of each molecule, Fig. 6a plots the DPV responses of DA to various concentrations of 0.2 – 70 μM in phosphate buffer solutions (0.1 M, pH 6.0) with a constant 40 μM EP at EY/GO/GCE. The result indicated that the cathodic peaks current of DA gradually increased with the concentration of DA increased. From the Fig. 6a inset, the linear regression equation was $I_{pc} (\mu\text{A}) = 0.1492C (\mu\text{M}) + 0.2037$ ($R = 0.990$) with the detection limit (LOD) of 0.05 μM ($S/N = 3$). Similar trend was found for EP with the presence of DA, Fig. 6b plots the DPV responses of EP to various concentrations in 0.1 M phosphate buffer solutions (pH 6.0) with a constant 30 μM EP. The reduction peak currents of EP were also linear with the EP concentration in the range of 0.2 – 70 μM , and the regression equation was $I_{pc} (\mu\text{A}) = 0.1948C (\mu\text{M}) + 0.3581$ ($R = 0.989$). The detection limit ($S/N=3$) was 0.03 μM for EP.

DPV of the simultaneous detection of EP and DA (Fig. 6c) was conducted with concentrations ranging from 0.2 to 100 μM . Two well-defined reduction peaks were observed. In addition, the good relationship between the reduction peak current and the DA/EP concentration were obtained. As seen in

the inset of Fig. 6c, the linear regression equations were $I_{pc} (\mu A) = 0.1373C (\mu M) + 0.0396$ ($R = 0.998$) for DA and $I_{pc} (\mu A) = 0.2083C (\mu M) + 0.3902$ ($R = 0.991$) for EP, respectively. From the linear regression equations, the detection limit was estimated to be 50 nM for DA and 30 nM for EP ($S/N = 3$), respectively. Moreover, Table 1 summarized the comparison of the electrochemical performance of two compounds detection at the proposed electrode with other reported sensors. As can be seen, the linear range and the detection limit of the obtained modified electrode were improved in some cases and was comparable with some of them [33, 35, 38-42]. It was manifested that the sensor presented in this work possessed excellent electrochemical performance, which had a promising prospect for the simultaneous detection of DA and EP.

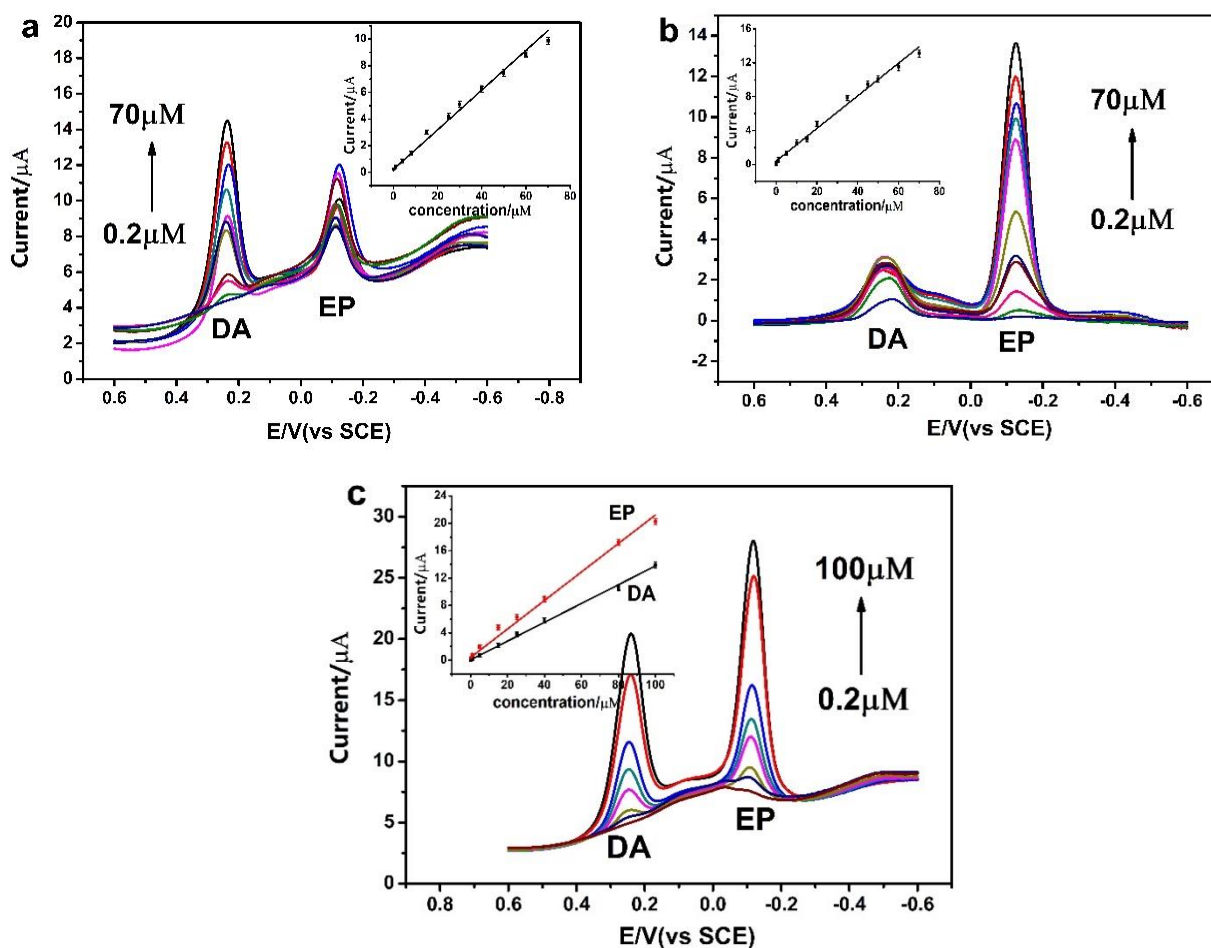


Figure 6. (a) DPV curves of EY/GO/GCE in 0.2, 1.0, 5.0, 10.0, 15.0, 20.0, 25.0, 35.0, 50.0, 60.0 and 70.0 μM DA solutions with the presence of 40 μM EP, inset: relationship of reduction peak current vs. concentration of DA. (b) DPV curves in 0.2, 1.0, 5.0, 10.0, 15.0, 20.0, 25.0, 35.0, 50.0, 60.0 and 70.0 μM EP solutions with the presence of 30 μM DA, inset: relationship of reduction peak current vs. concentration of EP. (c) DPV curves in the concentrations of the DA and EP, 0.2, 1.0, 5.0, 10.0, 25.0, 40.0, 80.0 and 100.0 μM , inset: the calibration curves of DA and EP.

To evaluate the selectivity of the EY/GO modified electrode. The possible interferences of other compounds were also investigated at the modified electrode. Some foreign species were added into phosphate buffer (0.1 M, pH 6.0) containing 10 μM DA and 10 μM EP. Different concentration of

histamine (100 μM), uric acid (30 μM), tyramine (30 μM), L-cysteine (60 μM), tryptamine (300 μM), glucose (1.5 mM), H_2O_2 (1.5 mM) and ascorbic acid (1 mM) had no evident effect on determination of DA and EP (signals change below 5%), demonstrating the good selectivity of the modified electrode for the further application.

Table 1. Comparison of performances of different sensors for simultaneous detection of EP and DA.

Materials	Linear		Detection		Reference
	range (μM)		limit (μM)		
	DA	EP	DA	EP	
AgNP/SiO ₂ /GO/GCE ^a	2.0-80.0	0.23-83.3	0.26	0.27	[8]
poly(isonicotinic acid)/CPE	80-700	5-100	20.0	1.0	[33]
B-MWCNTs/AuNPs/GCE ^b	323-1020	323-1020	0.20	0.30	[35]
PAIUCPE ^c	0.8-300	2.0-150	0.17	0.32	[38]
α -CD/CNT/GCE ^d	2.0-1000	.0-150	1.0	0.5	[39]
Poly(taurine)/GCE	1.0-800	2.0-600	0.1	0.3	[40]
Poly(DA)- nanogold/GCE ^e	1.0-80	1.0-80	0.08	0.1	[41]
Poly-FA/MWCNT/GCE ^f	5.0-120	73-1406	2.21	22.28	[42]
EY/GO/GCE	0.2-100	0.2-100	0.05	0.03	This work

^a: mesoporous silica nanoparticles, graphene and silver nanoparticles; ^b: boron-doped multi-walled carbon nanotubes/gold nanoparticles; ^c: pre-anodized inlaying ultrathin carbon paste electrode; ^d: α – cyclodextrin and carbon nanotubes; ^e: polydopamine and gold nanoparticles; ^f: poly ferulic acid /multi-walled carbon nanotubes.

3.6 Reproducibility and stability of EY/GO/GCE

The reproducibility of the EY/GO modified electrode was evaluated in 50 μM DA and 50 μM EP solutions by using six different electrodes prepared under the same conditions, and the relative standard deviation (*RSD*) of their electrochemical responses was measured to be only 3.44% to DA and 2.61% for EP, respectively. In order to examine the stability of the modified electrode, after two weeks of storage at refrigerator, it retained about 86.7% of their initial current value, suggesting the excellent stability of the proposed electrode.

3.7 Real samples analysis

A recovery test was conducted to evaluate the practical efficiency of the proposed EY/GO/GCE by the standard addition method. The application of the sensor for the detection of DA and EP in the real samples such as human urine was investigated. The recovery was studied by spiking certain amounts of DA and EP. The results were summarized in Table 2. The recoveries were 95.3–106.5 % for the two

compounds, indicating that the EY/GO/GCE was efficient and sensitive for the assay of DA and EP in real biological samples.

Table 2. Determination of DA and EP in human urine samples on EY/GO/GCE (n=3)

Sample	Analyte	Added (μM)	Found ^a (μM)	RSD ^b (%)	Recovery ^c (%)
Urine 1	DA	10	9.76 \pm 0.28	2.9	97.6
	EP	10	11.53 \pm 0.22	1.9	115.3
Urine 2	DA	20	21.30 \pm 0.42	2.0	106.5
	EP	20	19.05 \pm 0.53	2.8	95.3

^a Standard addition method. ^b Relative standard deviation for 3 successive measurements.

4. CONCLUSION

In this work, a glassy carbon electrode modified with eosin Y by electro-deposition on the surface of coating GO modified electrode was successfully proposed and applied for the sensitive and selective detection of DA and EP. The EY/GO/GCE enhanced the reduction peak currents towards DA and EP and the positive shift of the reduction peak potentials. The improving electrochemical performance was attributed to the synergistic effect of GO and EY with large surface area and high conductivity. The proposed EY/GO/GCE achieved high selectivity, long-time stability and good reproducibility for DA and EP. Moreover, the obtained sensor successfully detected the concentration of DA and EP in real urine samples.

ACKNOWLEDGEMENTS

This work was supported by National Natural Science Foundation of China (21904004), the Domestic visiting scholar program for outstanding young talents of Anhui Province (gxgnfx2019019), and the stable talent program and the outstanding talent program of Anhui Science and Technology University and Innovation and Entrepreneurship Training Program of Anhui Province (No. S201910879293).

References

1. F. Mora, G. Segovia, A.A. Del, B.M. De and P. Garrido, *Brain Res.*, 1476 (2012) 71.
2. N. Aslam, A. Kedar, H.S. Nagarajarao, K. Reddy, H. Rashed and T. Cutts, *Am. J. Med. Sci.*, 2 (2015) 81.
3. F. Xu, M.N. Gao, L. Wang, G.Y. Shi, W. Zhang and L.T. Jin, *Talanta*, 55 (2001) 329.
4. E. Grouzmann, O. Tschopp, F. Triponez, M. Matter, S. Bilz and M. Brandle, *Plos One.*, 10 (2015) 1.
5. S. Hu, Q. Huang, Y. Lin, C. Wei, H. Zhang, W. Zhang, Z. Guo, X. Bao, J. Shi and A. Hao, *Electrochim. Acta*, 130 (2014) 805.
6. S. Tufi, M. Lamoree, J. de Boer and P. Leonards, *J. Chromatogr. A.*, 1395 (2015) 79.

7. V. Sindelar, M. A. Cejas, F. M. Raymo, W. Z. Chen, S. E. Parker and A. E. Kaifer, *Chem.-Eur. J.*, 11 (2005)7054.
8. F.H. Cincotto, T.C. Canevari, A.M. Campos, R. Landers and S.A.S. Machado, *Analyst*, 139 (2014) 4634.
9. D. Brondani, C. W. Scheeren, J. Dupont and I. C. Vieira, *Analyst*, 137 (2012)3732.
10. D. Chen, H. B. Feng and J. H. Li, *Chem. Rev.*, 112(2012)6027.
11. S. Sreejith, X. Ma and Y. L. Zhao, *J. Am. Chem. Soc.*, 134(2012)17346.
12. K.A. Mkhoyan, A.W. Contryman, J. Silcox, D.A. Stewart, G. Eda, C. Mattevi, S.Miller and M. Chhowalla, *Nano Lett.*, 9 (2009) 1058.
13. G.M. Scheuermann, L. Rumi, P. Steurer, W. Bannwarth and R. Mulhaupt, *J. Am.Chem. Soc.*, 131 (2009) 8262.
14. A. Erdem, M. Muti, P. Papakonstantinou, E. Canavar, H. Karadeniz, G. Congur and S. Sharma, *Analyst*, 137 (2012) 2129.
15. L. Zhang, H. Cheng, H. Zhang and L. Qu, *Electrochim. Acta*, 65 (2012) 122.
16. F. Schedin, A.K. Geim, S.V. Morozov, E.W. Hill, P. Blake, M.I. Katsnelson and K.S. Novoselov, *Nat. Mater.*, 6 (2007) 652.
17. R.S. Sundaram, C.G. Navarro, K. Balasubramanian, M. Burghard and K. Kern, *Adv. Mater.*, 20 (2008) 3050.
18. J.T. Robinson, F.K. Perkins, E.S. Snow, Z.Q. Wei and P.E. Sheehan, *Nano Lett.*, 8 (2008) 3137.
19. Y. Wang, Y.M. Li, L.H. Tang, J. Lu and J.H. Li, *Electrochem. Commun.*, 11 (2009) 889.
20. A.J.S. Ahammad, M.M. Rahman, G.R. Xu, S.H. Kim and J.J. Lee, *Electrochim. Acta*, 56 (2011) 5266.
21. W.X. Cheng, P. Liu, M. Zhang, J.Z. Huang, F.L. Cheng and L.S. Wang, *RSC Adv.*, 7(2017) 47781.
22. J. Tang, W. Wang, S.B. Zheng, Y. Zhang, J.M. Wei and J.F. Wang, *Food Anal. Methods*, 9 (2016) 3044.
23. Z.X. Zhu, W.T. Cong, P.H. Zhang, W.D. Ma, M. Liu, H.Z. He, J. K. Choi, L.T. Jin and X.K. Li, *Electrophoresis*, 31 (2010) 3450.
24. W.T. Cong, W.J. You, M. Chen, J. Ling, Z.X. Zhu, J.K. Choi, L. Jin and X.K. Li, *Analyst*, 137 (2012)1466.
25. W.T. Cong, S.Y. Hwang, L.T. Jin, H.Z. He and J.K. Choi, *Electrophoresis*, 31 (2010) 411.
26. S.X. Min and G.X. Lu, *J. Phys. Chem. C*, 116 (2012)19644.
27. J.Y. Xu, Y.X. Li, S.Q. Peng, G.X. Lu and S.B. Li, *Phys. Chem. Chem. Phys.*, 15 (2013) 7657.
28. J.H. He, R. Qiu, W. Li, S.H. Xing, Z.R. Song, Q. Li and S.T. Zhang, *Anal. Methods*, 6 (2014) 6494.
29. J. Tang, Y.Y. Mao, J.H. Guo, Z.R. Li, C. Zhang and B.K. Jin, *Food Anal. Methods*, 11 (2018) 3380.
30. P.S. Ganesh and B.E. Kumara Swamy, *J. Mol. Liq.*, 220 (2016) 208.
31. W. Hummers and R.E. Offeman, *J. Am. Chem. Soc.*, 80(1958) 1339.
32. J.B. Zhang, L.N. Sun and T.K. Yoshida, *J. Electroanal. Chem.*, 662 (2011)384.
33. Y. Z. Zhou, L.J. Zhang, S. L. Chen, S. Y. Dong and X. H. Zheng, *Chin. Chem. Lett.*, 20 (2009) 217.
34. S.B. Zheng, R. Huang, X.Q. Ma, J. Tang, Z.R. Li, X.C. Wang, J.M. Wei and J.F. Wang, *Int. J. Electrochem. Sci.*, 13 (2018) 5723.
35. N. G. Tsierkezos, U. Ritter, Y. N. Thaha, A. Knauer, D. Fernandes, A. Kellarakis and E. K. McCarthy, *Chem. Phys. Lett.*, 710(2018) 157.
36. J. Tashkhourian, S.F. Nami-Ana and M. Shamsipur, *J. Mol. Liq.*, 266 (2018) 548.
37. W.J. Kang, L.M. Niu and L. Ma, *Chin. Chem. Lett.*, 20 (2009) 221.
38. J.E. Huo, J. Li and Q.M. Li, *Mater. Sci. Eng. C.*, 33(2013) 507.
39. G.Y. Wang, X.J. Liu, G.A. Luo and Z.H. Wang, *Chinese J. Chem.*, 23 (2005) 297.
40. Y. Wang and Z.Z. Chen, *Colloid Surface B.*, 74 (2009) 322.

41. Y. Zhang, W. Ren and S.L. Zhang, *Int. J. Electrochem. Sci.*, 8 (2013) 6839.
42. L. V. Silva, C. B. Lopes, W. C. Silva, Y. G. Paiva, F.A. Santos Silva, P. R. Lima, L. T. Kubot and M.O. F. Goulart, *Microchem. J.*, 133 (2017) 133.

© 2020 The Authors. Published by ESG (www.electrochemsci.org). This article is an open access article distributed under the terms and conditions of the Creative Commons Attribution license (<http://creativecommons.org/licenses/by/4.0/>).